New Astronomy 58 (2018) 96–106

Contents lists available at ScienceDirect

New Astronomy

journal homepage: www.elsevier.com/locate/newast

Lunar fingerprints in the modulated incoming solar radiation: *In situ* insolation and latitudinal insolation gradients as two important interpretative metrics for paleoclimatic data records and theoretical climate modeling

Rodolfo Gustavo Cionco[a,c,*], José Ernesto Valentini[a], Nancy Esther Quaranta[a,c], Willie W.-H. Soon[b]

[a] Grupo de Estudios Ambientales, Universidad Tecnológica Nacional, Colón 332, San Nicolás, Argentina
[b] Harvard-Smithsonian Center for Astrophysics, Cambridge, MA 02138, USA
[c] Comisión de Investigaciones Científicas de la Prov. de Buenos Aires (CIC), Argentina

HIGHLIGHTS

- A new and comprehensive *in situ* insolation and LIG forcing database for 2000+ years.
- Both orbital modulation and intrinsic TSI variation accounted for.
- Local insolation and LIG contain strong lunar nodal modulation fingerprints.
- Useful for modeling lunar signals in instrumental and paleoclimate proxies records.

ARTICLE INFO

Article history:
Received 15 July 2017
Revised 8 August 2017
Accepted 10 August 2017
Available online 12 August 2017

ABSTRACT

We present a new set of solar radiation forcing that now incorporated not only the gravitational perturbation of the Sun-Earth-Moon geometrical orbits but also the intrinsic solar magnetic modulation of the total solar irradiance (TSI). This new dataset, covering the past 2000 years as well as a forward projection for about 100 years based on recent result by Velasco-Herrera et al. (2015), should provide a realistic basis to examine and evaluate the role of external solar forcing on Earth climate on decadal, multidecadal to multicentennial timescales. A second goal of this paper is to propose both *in situ* insolation forcing variable and the latitudinal insolation gradients (LIG) as two key metrics that are subjected to a deterministic modulation by lunar nodal cycle which are often confused with tidal forcing impacts as assumed and interpreted in previous studies of instrumental and paleoclimatic records. Our new results and datasets are made publicly available for all at PANGAEA site.

© 2017 Elsevier B.V. All rights reserved.

1. Introduction

Cionco and Soon (2017) recently presented a new set of boundary conditions accounting for the short-term orbital forcing (STOF) effects valid over the full Holocene interval. But in that paper, we have adopted a time-invariant total solar irradiance (TSI) index in order to strictly focus on the planetary orbital perturbations on the incoming solar radiation. In this paper, we improve the realism for this key external boundary condition for understanding and evaluating the Earth climate variability by now incorporating a new estimate of a time varying TSI index as recently published by Velasco-Herrera et al. (2015). Although the time-varying TSI index proxy appears to be available for the past 9000 years or so (e.g., Steinhilber et al. 2009), we shall limit our current study to the past 2000 years because several papers (Roth and Joos 2013; Khider et al., 2014; Soon 2014) have recently criticized and challenged the Holocene TSI index proposed by Steinhilber et al. (2009). In addition Soon (2014) and Soon et al. (2014) highlighted that both the time history and amplitude for solar activity forcing over the full Holocene may be less well-constrained than normally assumed. We further restrict ourselves to the lunar nodal forcing scale of 18.6 years for the deterministic modulation of the incoming solar radiation while leaving other more complex modulation timescales that were recognized and discussed for example in Cionco and Soon (2015) and Yndestad and Solheim (2017) for future explorations.

* Corresponding author.
E-mail address: gcionco@frsn.utn.edu.ar (R.G. Cionco).

http://dx.doi.org/10.1016/j.newast.2017.08.003
1384-1076/© 2017 Elsevier B.V. All rights reserved.

A second purpose of this paper is to propose and explore a new interpretation of the lunar signals and fingerprints often found wanting in various instrumental records covering ocean temperature, rainfall, to sea level (Loder and Garrett 1978; Yasuda et al., 2006; McKinnell et al. 2007; Gratiot et al., 2008; Yndestad et al., 2008; Agosta 2013; Malherbe et al., 2014; Osafune et al., 2014; Spada et al., 2014; Hansen et al., 2015 and references therein) as well as in paleoclimatic records (Cook et al., 1997; Black et al., 2009; Yasuda 2009; Davis and Brewer 2011 and references therein). Both Munks and Bills (2007) and Ray (2007) explored a mechanistic understanding and interpretation of the lunar signals, particularly the lunar nodal modulation of 18.6 years and concluded that the typically assumed connection arising from enhanced tidal vertical mixing or other tidal impacts may be not only inadequate but likely improbable. Indeed Munk and Bills (2007) has highlighted that the obliquity modulation of tidal mixing of a few percent and associated modulation in the meridional overturning circulation may have a role comparable to the parallel obliquity modulation of insolation but the estimate "involves even more than the usual number of uncertainties found in climate speculations." (p. 135).We propose in this paper both the role of *in situ* insolation forcing (i.e., at high latitude zone like 65°N as originally proposed by Milanković, 1941) and latitudinal insolation gradients, LIG, as plausible alternative metrics that also contained the modulation imprints of the lunar nodal forcing. Our proposal is not new but in fact has been considered and studied by Munk and Bills (2007) and Davis and Brewer (2011). Yet we will revisit this topic afresh because of the new STOF orbital solutions we have recently produced and published for the benefit of interpretive frameworks and perhaps ultimate mechanistic modeling and representation of the physical connections.

In Section 2, we analyze the calculation of *in situ* insolation forcing as well as LIG, we also compare and contrast with the results produced by Davis and Brewer (2011). We show that these authors did not present the nominal LIG's absolute values but instead they plotted variances with respect to a fiducial value. In Section 3, we provide our basic results and discuss our interpretation of the calculated local insolation and LIG time series. In particular we demonstrate that, in turn of argued at long-term Milanković scales (Davis and Brewer 2009), at short time-scales there are also obliquity signals in LIG at December's solstice. In addition, we further discuss and seek connection and interpretation of climate variations on multidecades to multicenturies in terms of the latitudinal temperature gradients (LTG) explored previously by Lindzen (1994) and Soon and Legates (2013). The search for a physical connection between LIG and LTG is likely fruitful because the impacts of the incoming solar radiation on Earth's atmosphere and near-surface thermal regimes are likely to be more direct and are the fastest mechanism among other avenues of transport of heat flows within the Earth's coupled air-sea-land interfaces. Our conclusions are given in Section 4.

2. Calculations of daily *in situ* insolation and latitudinal insolation gradients (LIG)

Borisenkov et al. (1985) and Bertrand et al. (2002) were among the first to include both the orbital effects and intrinsic variability of TSI into the calculation of the external boundary condition of incoming solar radiation, but their works only cover 100 and 400 years of duration, respectively. In addition, at that time the physical understanding of the factors responsible for TSI variations were still in infancy, this is why our current calculation will serve as an important update for an increasingly more realistic nature of this key boundary condition for studying Sun–climate relationships.

LIG are a key feature of the external forcing of the climate system, with relevant implications at not only long but also relatively shorter temporal scales (Davis and Brewster 2009; Davis and Brewster 2011). LIG have not been formally defined in the literature; here we determine *daily* LIG between two latitudes, φ_1 and φ_2 as the difference:

$$\Delta_d(\varphi_1, \varphi_2) = W_{\varphi 1} - W_{\varphi 2}, \tag{1}$$

where W_φ is the mean-daily insolation (averaged over a whole rotational day) or mean-daily irradiance of the corresponding day ($\mathrm{W\,m^{-2}}$) at a specified latitude, it is given by:

$$W_\varphi = \frac{\mathrm{TSI}(t)}{\pi}\left(\frac{1\mathrm{au}}{a}\right)^2\left(\frac{1+e\cos(\lambda-\varpi)}{1-e^2}\right)^2(H_0\sin\varphi\ \sin\delta + \cos\varphi\ \cos\delta\ \sin H_0), \tag{2}$$

where TSI(t) is the total solar irradiance evaluated at 1 au (a fix distance at the Sun), but varying through the Sun–Earth orbital year; a is the Earth's semi-major axis; λ is the true solar orbital longitude; H_0 is the Sun's setting hour angle; e is the Earth's orbital eccentricity and ϖ is the perihelion longitude reckoned from the equinox *of the date*. In Eq. (2), the Earth's obliquity, ε, is present in the Sun's geocentric declination, δ, and in H_0 defined by:

$$\sin\delta = \sin\lambda\ \sin\varepsilon, \quad \text{and} \quad \cos(H_0) = -\tan\varphi\ \tan\delta. \tag{3}$$

Therefore, the obliquity signals and with additional modulation by the Moon, is relatively more subtle than precession or eccentricity signals. The strong assumption in Eq. (1) is that a complete whole day should be considered in the calculation of mean irradiances. This means that for a given observer, Eq. (2) needs to be evaluated with a λ value corresponding to the local noon. Although this assumption is part of the daily irradiation definition, yet it is a usual practice in paleoclimate studies to evaluate W_φ as a *continuous* function of solar orbital longitude; i.e., at an arbitrarily desired λ. In this case, it is the mean-irradiance at *different terrestrial longitudes* (but at the same terrestrial parallel φ) that is being considered. This assumption could have a non-negligible impact on latitudinal temperature gradient because latitudinal net radiation gradient is sensitive to distribution of land and water, which controls the total poleward heat and water vapor transport (see e.g., Stone 1978); hence, could be very sensitive to the assumed value of terrestrial longitude. By following Cionco and Soon (2017) we can be reassured that the correct true solar orbital longitude is set at noon for a particular observer (i.e., very near Greenwich meridian). Inside a particular day, the effect of selecting arbitrary λ values can produce differences in mean-daily irradiance up to $2.5\,\mathrm{W\,m^{-2}}$ (see Fig. 20 in Cionco and Soon 2017). Nevertheless, in order to stick to this standard practice in paleoclimatology and to check and validate our LIG definition, we calculate Eq. (2) as continuous function of longitudes.

We compare our results and contrast them with Davis and Brewer (2011)'s calculation in Figs. 1 and 2, where LIG at solstitial days ($\lambda = 90°, 270°$), between 60°N and 30°N are shown. Unlike Davis and Brewer (2011), these figures show *actual quantitative LIG values*, i.e., the absolute magnitude of LIG values, not relative LIG *variances*. Indeed, those authors show LIG but presented as variances or anomalies (i.e., an important point not clearly stated nor discussed in that paper perhaps because of the qualitative argument presented in that paper), i.e., as the difference between actual LIG and a mean or fiducial value at a certain arbitrary time or averaged over a time interval. This choice of LIG anomalies can be seen in Fig. 2, where the LIG for the period 1880–2017 minus the corresponding LIG but calculated at 1970, is presented for June solstitial day. We chose the 1970 value because this is the closest (i.e., as closely as our own assumption permits) we can emulate Davis and Brewer (2011)'s values of LIG. For December solstice, our values are similar to the estimates by those authors. Nevertheless an exact replication is impossible because they used a very different TSI reconstruction. As shown in Fig. 1 and will be discussed in

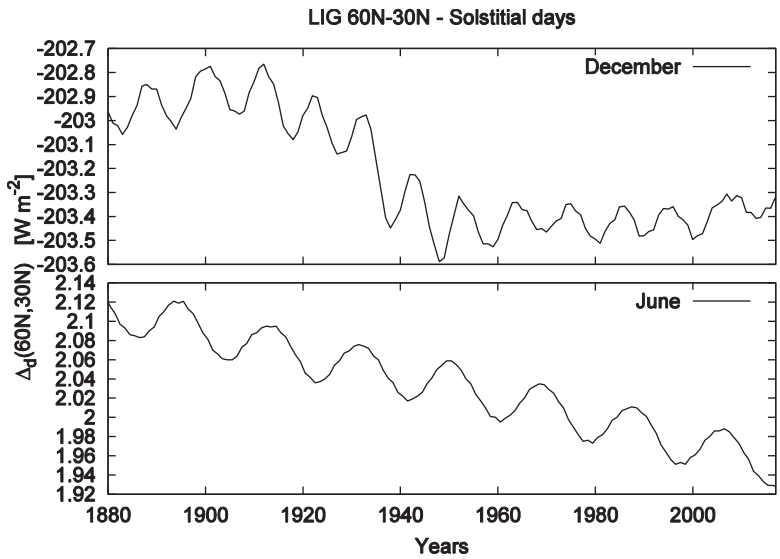

Fig. 1. LIG between 60°N and 30°N (Eq. (1)) after Davis and Brewster (2011) for solstitial days, with variable TSI incorporated. For December, the decadal band (~11-yr signal) of solar cycle is evident; whereas for June, the lunar nodal bidecadal (~19-yr) period is clearly shown.

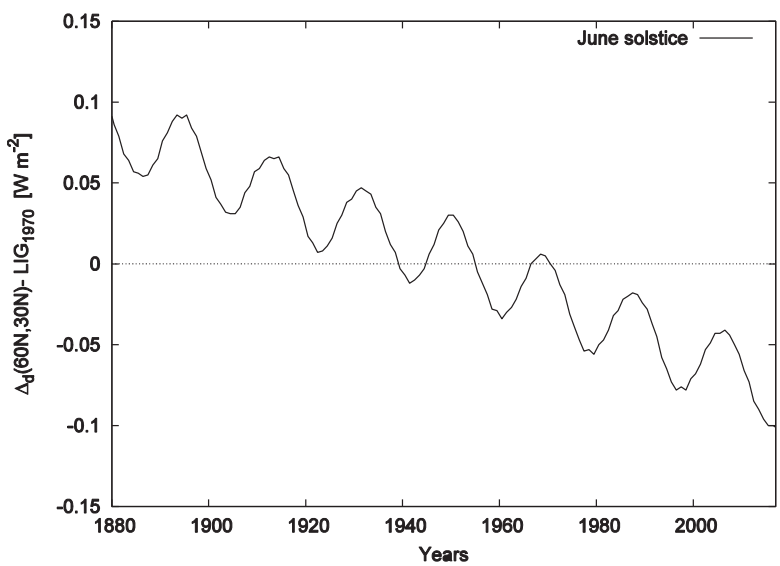

Fig. 2. Difference between LIG for June (i.e., Fig. 1) and the corresponding value at 1970 (LIG_{1970}) for the period 1880–2017. This comparison shows that Davis and Brewer (2011)'s LIG are presented as variances or anomalies, not absolute values.

more details later, TSI signal is very marked for December daily LIG at solstitial day. We conclude that if a physical representation or discussion of LIG is to prevail, as for example in the case of actual physical climate modeling, we must resist and avoid the confused representation of LIG in anomalies units as we re-highlighted in Fig. 2 here.

3. Results and discussion

3.1. Mean-daily irradiance forcing

Our *in situ* insolation forcings for an observer at 65°N (chosen traditionally following the physical reasoning given and motivated by Milanković 1941), including both STOF and TSI variations are shown in Figs. 3 and 4. They are presented as mean-daily insolation, given by Eq. (2), for equinoctial and solstitial days. For March equinox day, the secular march of precession is clearly seen as a linear trend and ongoing tendency. For September equinox, the effect is similar but of the opposite sign. This opposite-phasing feature between equinoctial insolation is the classical effect of precession (through ϖ and modulated by e), which constantly alters the Earth–Sun distance at the equinoxes (increasing one and decreasing the other). This effect on daily insolation can be demonstrated by evaluating Eq. (2) at equinoxes ($\lambda = 0°$, 180°), which at first order eccentricity (while neglecting the small oscillations in a) reads:

$$W_\varphi \propto \mathrm{TSI}(t)\,(1 \pm 2e\ \cos\varpi)\cos\varphi. \tag{4}$$

Where the plus sign holds for March, and minus for September; being the slope modulated by the latitude. As shown in Eq. (4), the dependence of W_φ on these orbital parameters at equinoxes, is proportional to $e\cos\varpi$. It is interesting to note that, at solstitial days, the dependence of W_φ changes is, in turn, on $e\sin\varpi$, then because of the accepted importance of daily insolation at June in Milanković theory, this quantity has been termed *climatic precession* (e.g, Hays et al., 1976). In addition, Fig. 3 shows the variations of solar TSI cycles, especially, the 11-yr Schwabe periodicity. We have taken into account the time-varying nature of TSI after

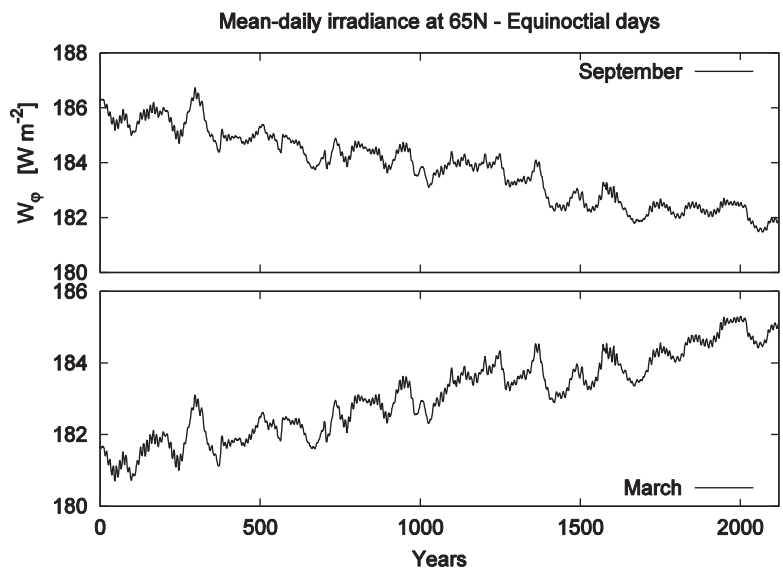

Fig. 3. Mean-daily irradiance (Eq. (2)) at 65°N for equinoctial days and variable TSI. In addition to long-term precession, the solar cycle (especially minor spikes of ~11-yr period) is clearly seen.

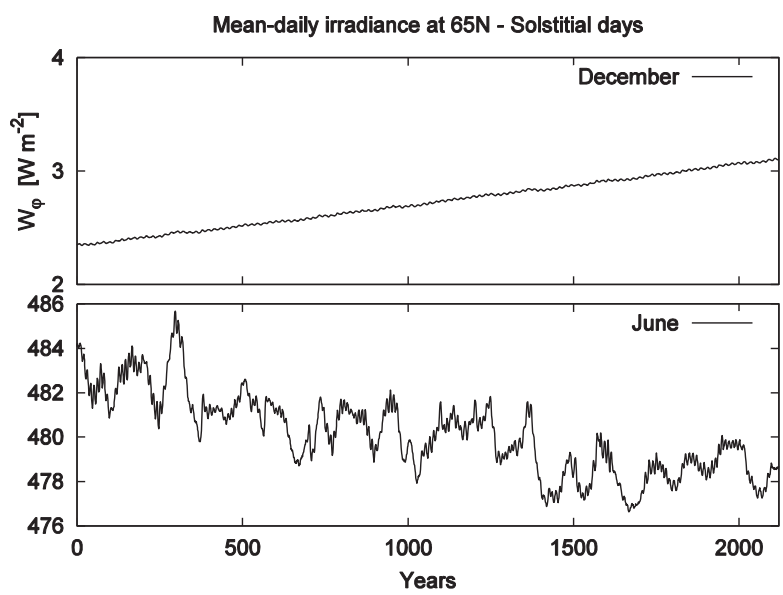

Fig. 4. Mean-daily irradiance (Eq. (2)) at 65°N for solstitial days and variable TSI. Precessional trend is strong in both plots. The 18.63-yr lunar signal is evidenced in December. In June the minor spikes seems to be more related to TSI's ~11-yr periodicity, but lunar signal is still present.

Velasco-Herrera et al. (2015) in this new set of calculations, between the years 0 (i.e., −1 BCE) and 2119. In fact, all the smasll spikes are due to this main periodicity, with a notorious absence of obliquity signals. This lack of evident lunar signal on equinoctial irradiance, can be demonstrated by inspecting Eq. (4), which is mathematically independent from obliquity. In such a scenario, *there is no lunar signal at equinoxes*.

The observed variations of TSI cycles are intrinsic to the nonlinear evolution of solar magnetic field over time; a subject we will avoid here but it is an important topic which has been extensively studied and recently reviewed (e.g., Charbonneau 2013; Cionco and Soon 2015; Weiss and Tobias 2016; Pipin 2017; Stefani et al., 2017).

All the results presented are, of course, also valid strictly also for Southern Hemisphere, out-phased by 6 months or 180° on solar orbital longitudes, then when we refer to season (summer–winter), a clarification note (NH) is added to indicate Northern Hemisphere season for which we are presenting the illustrative result here.

Fig. 4 shows the daily-mean irradiance at 65°N for both June and December solstices. Note that now, the lunar signal (18.63-yr) is clearly imprinted in December, but it is also present at June, mainly because the obliquity variations are more strongly present at solstices of high latitude locations (Cionco and Soon 2017). Nevertheless, at June, the oscillations of TSI signal are also strongly present, including the decadal (~11-yr) solar Schwabe band, which is clearly seen before year 2000, but after this year the lunar signal seems to be more prevalent. This ambiguity in both signals can be unveiled using the multitaper method (i.e., MTM; see Ghil et al., 2002), a method very powerful for not so long but noisy time series. Fig. 5 shows the MTM-power spectrum for mean-daily irradiance December solstice. The most important power derived from lunar-nodal signal, while the ~11-yr broad band of TSI modulation is also present, there are also shorter interannual spectral lines (lesser than 8-yr) that will be characterized in the next section. At June solstice (Fig. 6), in turn, the most important signal be-

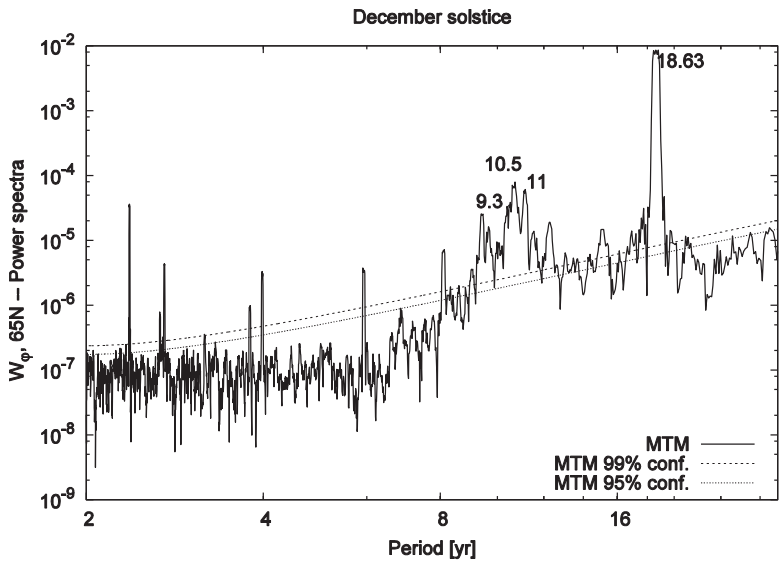

Fig. 5. MTM power spectrum of daily-mean irradiance at 65 N for winter solstice (NH). The lunar nodal signal is by far the most important periodicity (18.63-yr and 9.3-yr). The solar TSI cycle forcing is also visible at decadal (10.5–11-yr) band. Both the 95% and 99% significance levels above red-noise background spectrum are also indicated.

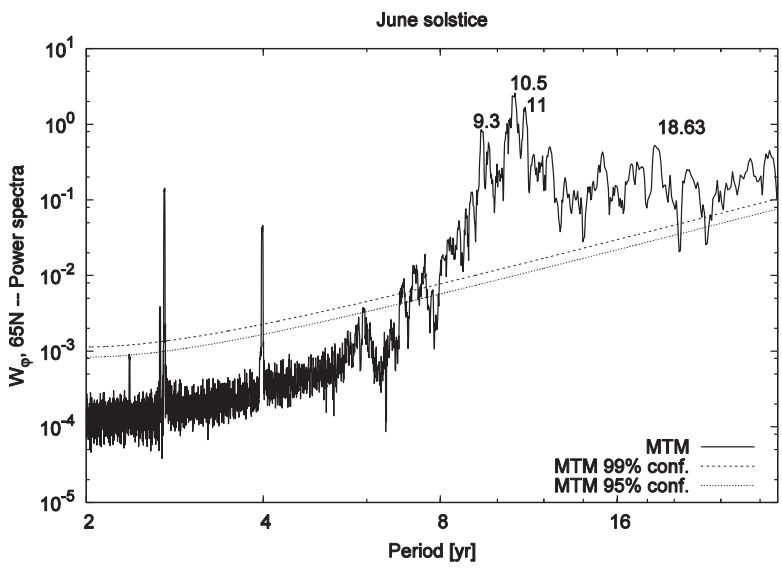

Fig. 6. MTM power spectrum of mean-daily irradiance at 65°N for summer solstice (NH). The solar TSI cycle forcing provides the most important power at decadal band. Nevertheless, obliquity signal is also present (as should be, because obliquity signal is also present at solstices). The other shortest periodicities have origins in the modulation by obliquity variations. Both the 95% and 99% significance levels above red-noise background spectrum are also indicated.

comes from solar intrinsic ~11-yr spectral band, but it is split into two peaks at 10.45 and 11-yr. Therefore, the interesting result of these pictures is that *solar TSI cycles can mask or attenuate lunar nodal signal at NH summer*. This empirical observation is important because W_φ at June is very often used as climate forcing in climate modeling or invoked in the interpretation of instrumental- and paleo-climatic records.

It is important to emphasize that different insolation quantities can be used as climate forcings, but daily-mean insolation at relatively high latitude like 65°N (which is also independent of the Earth rotation irregularities through the time) has been largely used, mainly because the quantity has both, precession (mainly) and also obliquity signal (see, e.g., Imbrie et al. 1982 for proposing insolation at 55°N rather than at 65°N in order to better account for both the obliquity and precession components of the orbital modulation) and other seasonal insolation forcings can be obtained from it by adding daily-mean insolation (Milanković 1941).

3.2. Daily latitudinal insolation gradients forcing

Figs. 7 and 8 show our daily LIG values (Eq. 1) computed between 60°N and 30°N (in the sense of 60 minus 30° in latitude), for equinoctial and solstitial days. Here it would be relevant to point out that both strengthening and weakening of the LIG are likely to find close correspondence in the LTG as examined in details by Lindzen (1994) and Soon and Legates (2013) as a key manifestation of climate dynamics operating on regional and hemispheric spatial scale and extent. The plausible fact is that warm global climate is mainly a consequence of weakening LIG and hence a corresponding weakening of LTG and vice versa for a cold glacial climatic environment where the LIG and LTG are both enhanced or strengthened nearly concurrently (see discussion and review by Lindzen 1994).

For equinoxes, the solar Schwabe cycle in TSI simply superposed on the more dominant effects of orbital precessional tendencies (see Fig. 7). At December solstice, as we have already seen

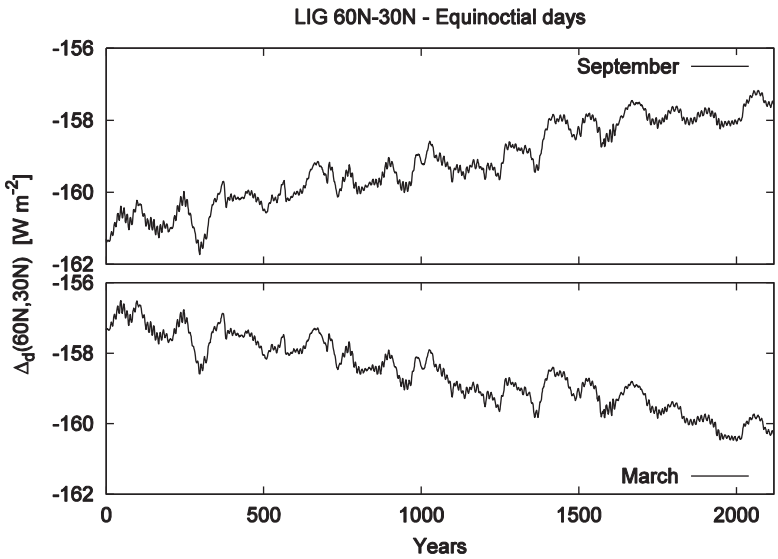

Fig. 7. LIG between 60°N and 30°N (Eq. (1)) for equinoctial days, with variable TSI incorporated. The precessional trend, with solar TSI cycles co-modulating the shorter-term variances, drives the main tendency in LIG values. The 11-yr signal of solar TSI cycle can be seen as minor spikes superposed on the longer-term trends.

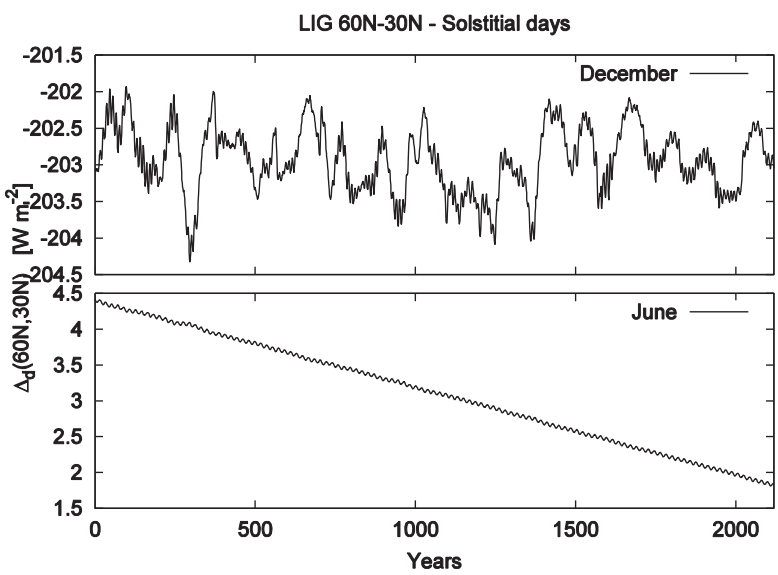

Fig. 8. LIG between 60°N and 30°N (Eq. (1)) for solstitial days, with variable TSI incorporated. The precessional effects cancel out at December, the solar TSI cycle periods exhibit a relatively larger modulating amplitudes for December solstice than during equinoxes. Nevertheless at June, long-term modulations of obliquity with the lunar-nodal 18.63-yr signal are visible.

in Fig. 2's presentation of the LIG for the 1880–2017 interval, the precession trends and tendencies are roughly cancelled out on this temporal domain, with the solar TSI modulation dominating the LIG expressions. For June, the long-term trend of obliquity and the lunar nodal 18.63-yr cycle can be very clearly seen. As a result, the differences in insolation at both latitudes provides a similar result/effect when compared to the *in situ* insolation metrics for equinoxes, but inverted. A similar result for solstices but interchanging winter by summer (NH), with the obliquity signal apparently cancelled-out on December and with the TSI signal weakly superposed on the precessional tendency at June.

Nevertheless, at NH winter the lunar signal is also present as can be demonstrated by spectral analysis using MTM method. First, Fig. 9 shows the MTM-power spectrum for the LIG at summer (NH) solstice. The periods arising from nutation modulation part of obliquity are clearly seen, with the lunar nodal cycle at 18.63-yr obviously dominant. At around the decadal band, the TSI signal is also present, but it is separated into two peaks at 10.45 and 11-yr. Taken into account the fact that Jupiter signal is also present (11.86-yr), the power at this decadal band is very considerable. At NH winters (Fig. 10), the lunar nodal period is attenuated, nevertheless the obliquity signal is still present and also the second harmonics of lunar node (9.3-yr) can also be clearly detected. In addition, at shorter timescales, short *nutational* periods are clearly seen. Then, lunar signal is relatively more subtle, with appreciable difference in its intensity, being evident in NH summer and weaker (but still present) in NH winter. For a full planetary description of these rather rich underlying orbital dynamics and periodicities, the reader is directed to Cionco and Soon (2017).

It is interesting to note that for winter LIG (NH) the precession signal is dominant at long-term Milanković scales (Davis and Brewer 2009); this fact has motivated geoscientist to say that at winter (NH), LIG is dominated by precession. In our new result, we demonstrate by spectral analysis, that at STOF timescales, the most important planetary signal *is obliquity* for winter (NH) but

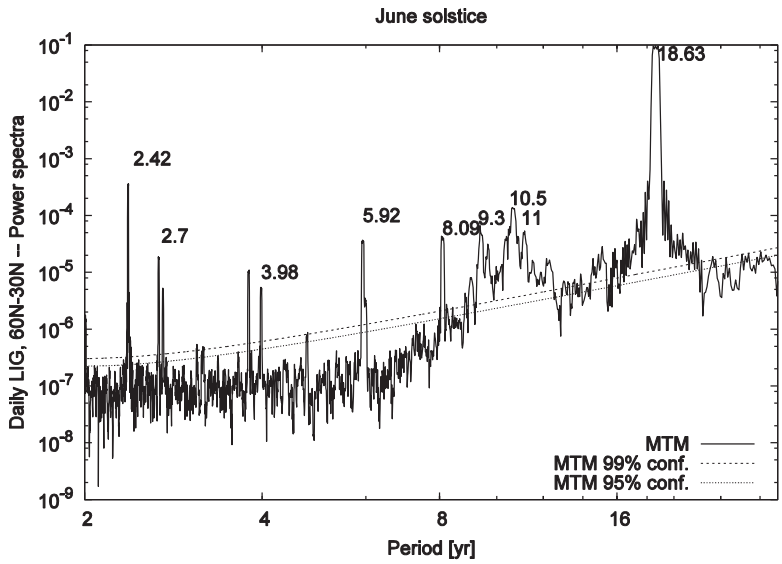

Fig. 9. MTM power spectrum of daily LIG between 60°N and 30°N at summer solstice (NH). The lunar nodal signal is by far the most important periodicity. The solar cycle forcing is also visible at decadal band. The other shortest periodicities have origins in the modulation by obliquity variations. Both the 95% and 99% significance levels above red-noise background spectrum are also indicated.

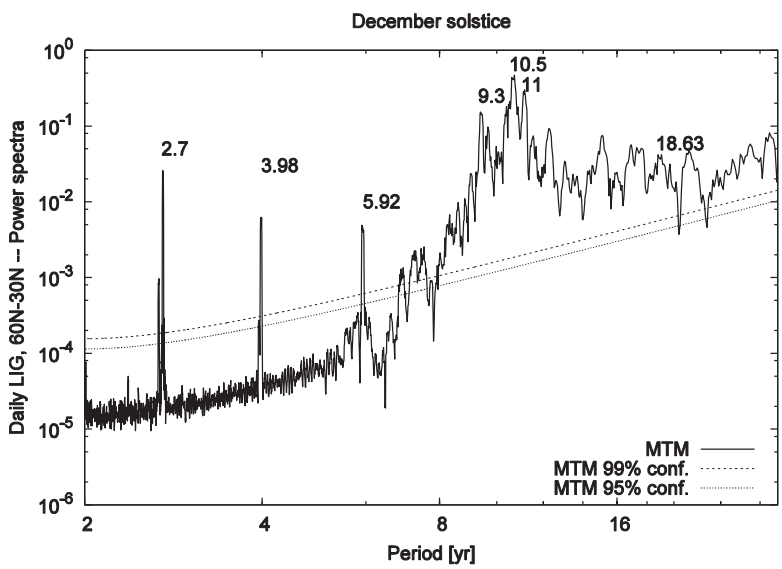

Fig. 10. MTM power spectrum of daily LIG between 60°N and 30°N at winter solstice (NH). The solar TSI cycle forcing provides the most important power at decadal band. Nevertheless, obliquity signal is also present (even the lunar nodal cycle) and its harmonic at 9.3 yr. The other shortest periodicities have origins in the modulation by obliquity variations. Both the 95% and 99% significance levels above red-noise background spectrum are also indicated.

with intrinsic solar TSI changes providing the most important and persistent modulation factor.

The time variation of the lunar modulation signals and the 11-yr period of solar Schwabe cycle through time, for both extremes of summer and winter solstices, is now assessed by using wavelet transform (Grinsted et al., 2004) for a proper time-frequency representation. Fig. 11 shows the lunar nodal signal persisting throughout the whole 2000+ years interval in comparison to the relative intermittency of the ~11-yr period of solar TSI cycle. We suggest that this fact concerning the very strong and persistent nature of lunar nodal modulation of both middle to high latitude mean-daily insolation and the LIG are clearly very attractive in terms of serving as an alternative explanation and interpretation to all the lunar signals observed in all the studies discussed in the introduction section. This new choice of alternative explanation and interpretation is especially attractive when one seriously weighed in the two very prominent results and opinion expressed recently in Munk and Bills (2007) and Ray (2007) in that they both proposed the tidal impacts in terms of any number of exact physical mechanisms like modulation of the vertical mixing rate in the pelagic ocean or coastal continental shelf to be unlikely to be real or of significant amplitudes. However, in our current preliminary study, we leave open the newly proposed and complex inter-connections through the persistent modulation of atmospheric tides by lunar forcing as recently explored by Wilson and Sidorenkov (2013) for the explanation of the standing-wave-like patterns of summer (DJF) mean sea level pressure and sea surface temperatures in the Southern Hemisphere.

Finally, we present detailed daily LIG calculation from year 2000 to 2119 forward projecting to the future (Figs. 12 and 13) for the same latitudes. For daily LIG a maximum is expected near 2060 at equinoctial days. The same expectation is seen for December solstice, with these maxima explained by the predicted solar cycle in TSI predicted. For June solstice the same long-term obliq-

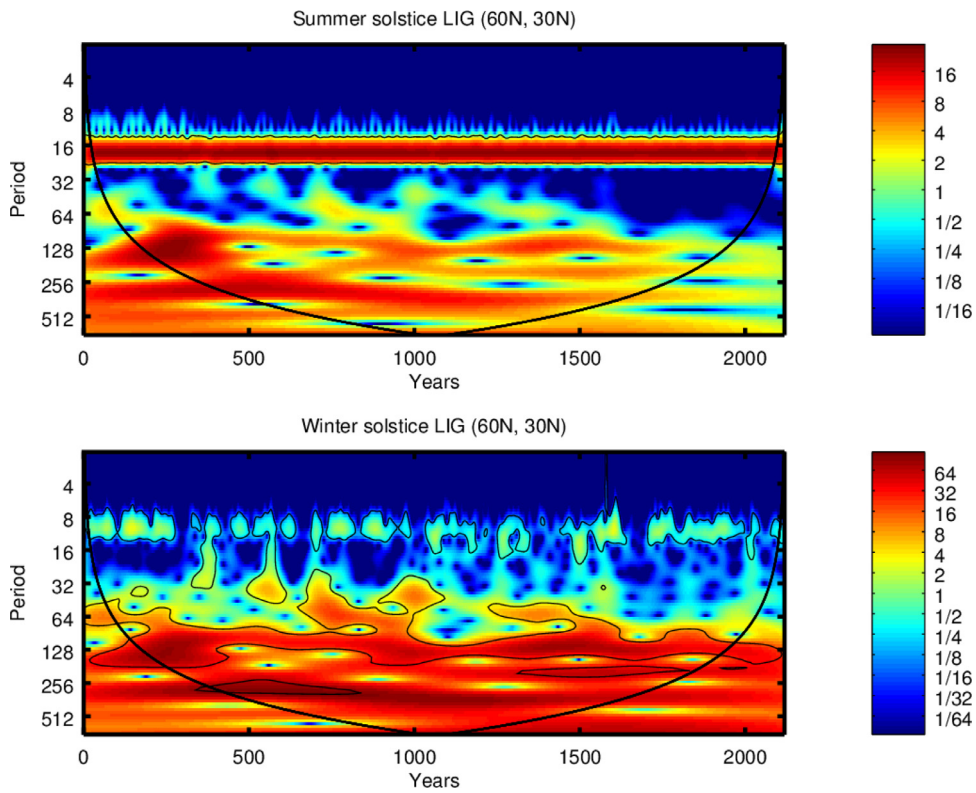

Fig. 11. Wavelet transform of daily LIG between 60°N and 30°N at sosticial days (NH). The persistency of lunar nodal cycle and the intermittency of 11-yr periodicity of solar cycle are evident. Several other periodicities around 60-yr, 80-yr, 120-yr and 240-yr are also found (i.e., Velasco Herrera et al. 2015; with the longer periods possibly related to intrinsic solar cycles studied in e.g., Soon et al., 2014). The cone of influence, where meaningful periodicities are found, is also marked.

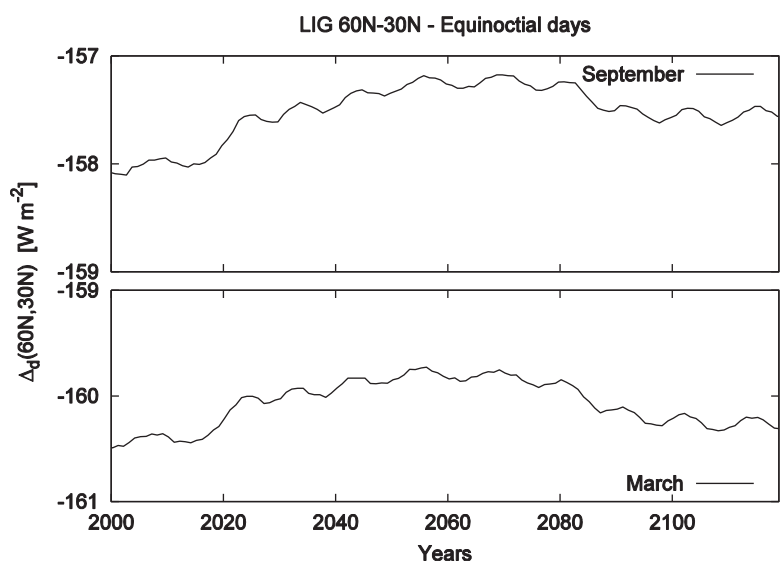

Fig. 12. LIG for the present time and the next 100 years or so, predicted by the forward integration of Sun-Earth orbits and TSI model used, at equinoctial days. Around 2060 an increase in latitudinal gradients is expected for both equinoxes.

uity decreasing trend is dominant and observed. This tendency is expected for June solstice because the solar Schwabe cycle signal is absent. We will keep the discussion of our results to the illustrative, bare minimum shown here in that we propose and invite all interested scientists to start utilizing our new database for any number of research investigation and activity. We simply wish to note that any realistic and comprehensive assessments of plausible future climatic forcing must include both the orbital as well as intrinsic solar magnetic modulation of the incoming solar radiation as outlined and described in this paper. This caution is important when considering the rather wide-spread rush to conclusion concerning the role of solar forcing and other natural and anthropogenic factors for climate in past and present literatures (see e.g., Budyko 1972; Broecker 1975 [1]; Budyko and Vinnikov 1976; Lean and Rind 2001; Lin and Sun 2007; Feulner and Rahmstorf 2010; Jones et al., 2012; Meehl et al., 2013; Abdussamatov 2015;

[1] In this particular rare case, the author corrected himself as presented in the later publication some 42 years later, see Broecker (2017).

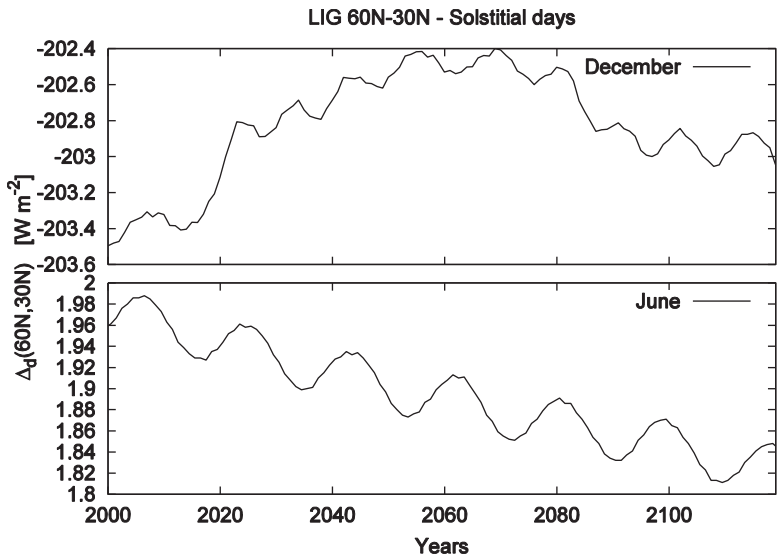

Fig. 13. LIG for the present and next 100 years or so, predicted by the forward integration of Sun-Earth orbits and TSI model used, at solstitial days. Around 2060 an increase in latitudinal gradients is expected for winter (NH) whereas for summer the ongoing, persistent obliquity tendency is seen.

Lüdecke and Weiss 2017; Matthes et al., 2017; Stozhkov et al., 2017; Zharkova et al., 2017).

4. Conclusions

We have provided a new set of external boundary conditions accounting for both the orbital effects and intrinsic magnetic variability of the Sun. This database should be profitable for all explorations related to the interpretation of paleoclimatic records and signals as well as the representation of the realistic mechanistic processes involved in the forcing-feedback paradigm of climatology. Here we argue that both the *in situ* mean-daily insolation and the LIG metrics are important for a fuller and more comprehensive study of how the changes of the external insolation forcing may trigger, sustain and modulate the local, regional and hemispheric scales of climate on decadal, multidecadal to centennial timescales. LIG which, in turns, can be closely associated with the modulation of LTG or the so-called equator-to-pole temperature gradient (Lindzen 1994; Soon and Legates 2013) that in turn represents a clear negative feedback on the broad, hemispheric scale. Local *in situ* mean-daily insolation clearly emulates the role imagined by Milanković but has been recently re-proposed and shown, for example, by Soon (2009) to play a key role for the Arctic-mediated modulation of the multidecadal to centennial scale climate variations observed using both available instrumental thermometer, rain-gauges and paleoclimatic proxies records.

For mean-daily irradiance, lunar nodal signal is always present at solstices, being dominant at winter (NH) but attenuated at summer (NH) by TSI decadal band. TSI variations are present at both equinoxes and solstices, but stronger at summer (NH) solstitial day. For daily LIG between high and low latitudes, the precession-induced trend superimposed by the solar TSI cycle drives the gradients at equinoxes. But at solstices, the solar TSI cycle is dominant at December; while in contrast the effect of lunar nodal cycles are strong and dominating at June. Nevertheless, at winter (NH) obliquity signal is the most important planetary signal present. This empirical fact, which is relevant for the shorter interannual, decadal to centennial timescales, defies the known findings for long-term Milanković scale, namely that precession (not obliquity) is dominant at winter (NH). Therefore, at STOF timescales, summer daily LIG (NH) is driven by lunar nodal modulation; whereas at winter (NH) the preponderant signal is TSI (11-yr and other longer-term bands as presented for example in Velasco Herrera et al. 2015). This lunar nodal signal at June is persistent along the full time interval of 2000+ years covered, whereas the main TSI signals at December solstice is only intermittent. The 11-yr TSI's band is always split into two peaks of 10.5-yr and 11-yr, showing the bi-modal occurrence of TSI cycles at decadal band.

For paleoclimate studies, researchers typically invoked only summer solstice insolation (i.e., local *in situ* forcing), which contains both precession and obliquity signals. Also summer daily LIG have been used, because it is argued that it has obliquity but only small and minimal precessional modulations. This is interesting because obliquity is a persistent signal in geologic data. Summer daily LIG, though important and directly relevant, cannot completely explain the global ice volume or other regional alkenone-sea surface temperature and benthic δ^{18}O records of the Pliocene–Pleistocene epochs some 4 million years in duration (Raymo and Nisancioglu 2003; Liu and Herbert 2004; Bierley et al., 2009). Here we show that, at shorter (STOF) timescales, even the winter LIG has significant obliquity (nutational) imprints, which could have a similar effect on climate but at much shorter timescales, through the modulation and pacing of the meridional fluxes of heat and moisture (see the early discussion in Soon 2009). Here one must also pay attention to the fact that LIG values and the corresponding LTG changes are relatively stronger during winters when compared to other seasons. Nevertheless, the lunar nodal effect is weak against the 11-yr spectral band of intrinsic TSI forcing for the winter (NH) solstice. Therefore all these solar-intrinsic and lunar-planetary effects should be considered altogether for a fully comprehensive description of the latitudinal insolation forcing at each season.

In assessing the comparative magnitude of daily LIG gradients, we showed that LIG for other latitudes and regions can be considered as climatic forcing as well because their magnitudes are often bigger than June daily LIG. The mean-daily insolation at summer solstice (NH) is the most important forcing while daily LIG at June is relatively smaller and hence a weaker role. In addition, we have shown that daily LIG published in Davis and Brewer (2011) are LIG variances or anomalies (which is not clearly stated nor justified in that paper). This objective highlight by our current study is important because an unprepared reader or climate modeler may misconstrued the results to represent the actual magnitude of daily LIG which are clearly a more directly relevant and necessary met-

ric in order to quantify the climate effects and responses to any modulation of the LIG or to connect to the concurrently occurring modulation in LTG as discussed in Lindzen (1994).

Finally, we wish to add that all our discussion, though focused on Northern Hemisphere as mere traditional illustrative examples, is also strictly valid and applicable for Southern Hemisphere as well. Our *in situ* insolation and LIG values will be directly applicable for a more systematic study and interpretation of the recent results shown for examples by Agosta (2013) and Malherbe et al. (2014) concerning the lunar nodal fingerprints found in the rainfall records in subtropical Andes, South America and subtropical South Africa, respectively. Also Whitlock et al. (2007) have argued for the importance of *in situ* insolation and LIG changes in modulating the complex interactions among fire-climate-vegetation variables within the southern South America. In effects, these authors found that the weakened LTG during the relative warm early-to-mid Holocene interval were accompanied by relatively weaker westerlies and a southward shift of the prevailing storm tracks and hence a more vigorous fire regime when compared to the late Holocene period. If such an empirical relation were to hold true for present time, one would imagine consulting the LIG values and tendencies to forecast the corresponding LTG and weather pattern responses in order to evaluate the multi-dimensional relations with contemporary anthropogenic factors.

Our numerical results for the local insolation and LIG and complimentary notes to Grinsted et al. (2004)'s wavelet package `Octave` are available on PANGAEA repository: https://doi.pangaea.de/10.1594/PANGAEA.877817

Acknowledgment

We thank Professor Victor Velasco Herrera for sharing his historical TSI reconstruction and future TSI projection records. The authors acknowledge the support of the grant UTN-4362 "Irradiación Solar Recibida para Lapsos Intraanuales de Tiempo con especial énfasis en América del Sur" (2017–2018) of the Universidad Tecnológica Nacional, Argentina. JEV acknowledges BINID's UTN fellowship. WS's work was indirectly supported by SAO grant proposal ID 000000000003010-V101. RGC and WS contributed nearly equally on this paper.

References

Abdussamatov, H., 2015. Current long-term negative average annual energy balance of the Earth leads to the new Little Ice Age. Therm. Sci. 19 (Suppl. 2), S279–S288.
Agosta, E.A., 2013. The 18.6-year nodal tidal cycle and the bi-decadal precipitation oscillation over the plains to the east of subtropical Andes, South America. Int. J Climatol. 34 (5), 1606–1614.
Bertrand, C., Loutre, M.F., Berger, A., 2002. High frequency variations of the Earth's orbital parameters and climatic change. Geophys. Res. Lett. 29. doi:10.1029/2002GL015622.
Bierley, C.M., Fedorov, A.V., Liu, Z., Herbert, T.D., Lawrence, K.T., LaRiviere, J.P., 2009. Greatly expanded tropical warm pool and weakened Hadley circulation in the early Pliocene. Science 323, 1714–1718.
Black, D.E., Hameed, S., Peterson, L.C., 2009. Long-term tidal cycle influence on a late-Holocene clay minerology record from the Cariaco Basin. Earth Planet. Sci. Lett. 279, 139–146.
Borisenkov, Y.P., Tsvetkov, A.V., Eddy, J.A., 1985. Combined effects of Earth orbit perturbations and solar activity on terrestrial insolation: part I: sample days and annual mean values. J. Atmos. Sci 42, 933–940.
Broecker, W.S., 1975. Climatic change: are we on the brink of a pronounced global warming? Science 189, 460–463.
Broecker, W.S., 2017. When climate change predictions are right for the wrong reasons. Clim. Change 142, 1–6.
Budyko, M.I., 1972. The future climate. Eos Trans. Am. Geophys. Union 53 (10), 808–874.
Budyko, M.I., Vinnikov, K.Ya., 1976. Global warming. Sov. Meteorol. Hydrol. 7, 12–20.
Charbonneau, P., 2013. Chapter 3: dynamo models of the solar cycle. In: *Solar and Stellar Dynamos*, Saas-Fee Advanced Course, 39. Springer-Verlag, Berlin Heidelberg, pp. 87–151.
Cionco, R.G, Soon, W., 2015. A phenomenological study of the timing of solar activity minima of the last millennium through a physical modelling of the Sun–planets interaction. New Astron. 34, 164–171.
Cionco, R.G, Soon, W., 2017. Short-term orbital forcing: a quasi-review and a reappraisal of realistic boundary conditions for climate modeling. Earth-Sci. Rev. 166, 206–222.
Cook, E.R., Meko, D.M., Stockton, C.W., 1997. A new assessment of possible solar and lunar forcing of the bidecadal drought rhythm in the Western United States. J. Clim. 10, 1343–1356.
Davis, B.A.S., Brewer, S., 2009. Orbital forcing and role of the latitudinal insolation/temperature gradient. Clim. Dyn. 32, 143–165.
Davis, B.A.S., Brewer, S., 2011. A unified approach to orbital, solar, and lunar forcing based on the Earth's latitudinal insolation/temperature gradient. Quat. Sci. Rev. 30, 1861–1874.
Feulner, G., Rahmstorf, S., 2010. On the effect of a new grand minimum of solar activity on the future climate on Earth. Geophys. Res. Lett. 37, L05707. doi:10.1029/2010GL042710.
Ghil, M., Allen, M.R., Dettinger, M.D., Ide, K., Kondrashov, D., Mann, M.E., Yiou, P., 2002. Advanced spectral methods for climatic time series. Rev. Geophys. 40 (1), 1–41.
Gratiot, N., Anthony, E.J., Gardel, A., Gaucherel, C., Proisy, C., Wells, J.T., 2008. Significant contribution of the 18.6 year tidal cycle to regional coastal changes. Nat. Geosci. 1, 169–566.
Grinsted, A., Moore, J.C., Jevrejeva, S., 2004. Application of the cross wavelet transform and wavelet coherence to geophysical time series. Nonlinear Processes Geophys. 11, 561–566.
Hansen, J.M., Aagaard, T., Kuijpers, A., 2015. Sea level forcing by synchronization of 56- and 74-year oscillations with Moon's nodal tide on the northwest European shelf (eastern North Sea to central Baltic Sea). J. Coastal Res. 31, 1041–1056.
Hays, J.D., Imbrie, J., Shackleton, N.J., 1976. Variations in the Earth's orbit: pacemaker of the ice ages. Science 194 (4270), 1121–1132.
Imbrie, J., 1982. Astronomical theory of the Pleistocene ice ages: a brief historical review. Icarus 50 (2–3), 408–422.
Jones, G.S., Lockwood, M., Stott, P.A., 2012. What influence will future solar activity changes over the 21st century have on projected global near-surface temperature changes? J. Geophys. Res. 117, D05103. doi:10.1029/2011JD017013.
Khider, D., Jackson, C.S., Stott, L.D., 2014. Assessing millennial-scale variability during the Holocene: a perspective from the western Tropical Pacific. Paleoceanography 29, 143–159. doi:10.1002/2013PA002534.
Lean, J., Rind, D., 2001. Earth's response to a variable Sun. Science 292, 234–236.
Lin, Z.-S., Sun, X., 2007. Multi-scale analysis of global temperature changes and trend of a drop in temperature in the next 20 years. Meteorol. Atmos. Phys. 95, 115–121.
Lindzen, R.S., 1994. Climate dynamics and global change. Annu. Rev. Fluid Mech. 26, 353–378.
Liu, Z., Herbert, T.D., 2004. High-latitude influence on the eastern equatorial Pacific climate in the early Pleistocene epoch. Nature 427, 720–723.
Loder, J.W., Garrett, C., 1978. The 18.6-year cycle of sea surface temperature in shallow seas due to variations in tidal mixing. J. Geophys. Res. 83 (C4), 1967–1970.
Lüdecke, H.-J., Weiss, C.-O., 2017. Harmonic analysis of worldwide temperature proxies for 2000 years. Open Atmos. Sci. J. 11, 44–53.
Malherbe, J., Engelbrecht, F.A., Landman, W.A., 2014. Response of the Southern Annular Mode to tidal forcing and the bidecadal rainfall cycle over subtropical southern Africa. J. Geophys. Res. 119, 2032–2049. doi:10.1002/2013JD021138.
Matthes, K., Funke, B., Andersson, M.E., et al., 2017. Solar forcing for CMIP6 (v3.2). Geosci. Model Dev. 10, 2247–2302.
McKinnell, S.M., Crawford, W.R., 2007. The 18.6-year lunar nodal cycle and surface temperature variability in the Northeast Pacific. J. Geophys. Res. 112. doi:10.1029/2006JC003671.
Meehl, G.A., Arblaster, J.M., Marsh, D.R., 2013. On the effect of a new grand minimum of solar activity on the future climate on Earth. Geophys. Res. Lett. 40, 1789–1793. doi:10.1002/grl.50361.
Milankovitch, M., 1941. Canon of Insolation and the Ice Age Problem. Israel Program for Scientific Translations, Jerusalem, pp. 1–484. 1969.
Munk, W., Bills, B., 2007. Tides and the climate: some speculations. J. Phys. Oceanogr. 37, 135–147.
Osafune, S., Masuda, S., Sugiura, N., 2014. Role of the oceanic bridge linking the 18.6 year modulation of tidal mixing and long-term SST change in the North Pacific. Geophys. Res. Lett. 41, 7284–7290. doi:10.1002/2014GL061737.
Pipin, V.V., 2017. Non-linear regimes in mean-field full-sphere dynamo. Mon. Not. R. Astron. Soc. 466, 3007–3020.
Ray, R.D., 2007. Decadal climate variability: is there a tidal connection? J. Clim. 20, 3542–3562.
Raymo, M.E., Nisancioglu, K., 2003. The 41 kyr world: Milankovitch's other unsolved mystery. Paleoceanography 18. doi:10.1029/2002PA000791.
Roth, R., Joos, F., 2013. A reconstruction of radiocarbon production and total solar irradiance from the Holocene ^{14}C and CO_2 records: implications of data and model uncertainties. Clim. Past 9, 1879–1909.
Soon, W., 2009. Solar Arctic-mediated climate variation on multidecadal to centennial timescales: Empirical evidence, mechanistic explanation, and testable consequences. Phys. Geogr. 30, 144–184.
Soon, W., 2014. Sun shunned. In: Moran, A. (Ed.), Climate Change—The Fact 2014. Institute of Public Affairs, pp. 57–66.
Soon, W., Legates, D.R., 2013. Solar irradiance modulation of Equator-to-Pole (Arctic) temperature gradients: empirical evidence for climate variation on multi--decadal timescales. J. Atmos. Solar 93, 45–56.

Soon, W., Velasco Herrera, V.M., Selvaraj, K., Traversi, R., Usoskin, I., Chen, C.-T.A., Lou, J.-Y., Kao, S.-J., Carter, R.M., Pipin, V., Severi, M., Becagli, S., 2014. A review of Holocene solar-linked climatic variation on centennial to millennial timescales: physical processes, interpretive frameworks and a new multiple cross-wavelet transform algorithm. Earth-Sci. Rev. 134, 1–15.
Spada, G., Galassi, G., Olivieri, M., 2014. A study of the longest tide gauge sea-level record in Greenland. Global Planet. Change 118, 42–51.
Stefani, F., Giesecke, A., Weber, N., Weier, T., 2017. On the synchronizability of the Tayler-Spruit and Babcock-Leighton type of dynamos. Solar Phys. submitted.
Steinhilber, F., Beer, J., Fröhlich, C., 2009. Total solar irradiance during the Holocene. Geophys. Res. Lett. 36 (19).
Stone, P.H., 1978. Constraints on dynamical transports of energy on a spherical planet. Dyn. Atmos. Oceans 2 (2), 123–139.
Stozkhov, Y.I., Bazilevskaya, G.A., Makhmutov, V.S., Svirzhevsky, N.S., Svirzhevskaya, A.K., Logachev, V.I., Okhlopkov, V.P., 2017. Cosmic rays, solar activity, and changes in the Earth's climate. Bull. Russ. Acad. Sci. 81, 252–254.
Velasco Herrera, V.M., Mendoza, B., Velasco Herrera, G., 2015. Reconstruction and prediction of the total solar irradiance: from the medieval warm period to the 21st century. New Astron. 34, 221–233.
Weiss, N.O., Tobias, S.M., 2016. Supermodulation of the Sun's magnetic activity: the effects of symmetry changes. Mon. Not. R. Astron. Soc. 456, 2654–2661.
Whitlock, C., Moreno, P.I., Bartlein, P., 2007. Climatic controls of Holocene fire patterns in southern South America. Quat. Res. 68 (1), 28–36.
Wilson, I.R.G., Sidorenkov, N.S., 2013. Long-term lunar atmospheric tides in the Southern Hemisphere. Open Atmos. Sci. J. 7, 51–76.
Yasuda, I., 2009. The 18.6-year period moon-tidal cycle in Pacific Decadal Oscillation reconstructed from tree-rings in western North America. Geophys. Res. Lett. 36. doi:10.1029/2008GL036880.
Yasuda, I., Osafune, S., Tatebe, H., 2006. Possible explanation linking 18.6-year period nodal tidal cycle with bi-decadal variations of ocean and climate in the North Pacific. Geophys. Res. Lett. 33. doi:10.1029/2005GL025237.
Yndestad, H., Solheim, J.-E., 2017. The influence of solar system oscillation on the variability of the total solar irradiance. New Astron. 51, 135–152.
Yndestad, H., Turrell, W.R., Ozhigin, V., 2008. Lunar nodal tide effects on variability of sea level, temperature, and salinity in the Faroe-Shetland Channel and the Barents Sea. Deep-Sea Res. I 55, 1201–1217.
Zharkova, V.V., Shepherd, S.J., Popova, E., and Zharkov, S.I. (2017) "Reinforcing the double dynamo model with solar-terrestrial activity in the past three millennia", astro-ph preprint, arXiv:1705.04482v2.